

## Article

# Study on Mechanical Characteristics of Deformation and the Failure of Gas-Containing Coal in the Wuhai Mining Area of China under Different Gas Pressure Conditions

Yejiao Liu <sup>1</sup>, Hui Xing <sup>2</sup>, Zeyu Duan <sup>1,\*</sup>, Chaoyun Yu <sup>3</sup>, Zhichao Tian <sup>3</sup> and Ting Teng <sup>1</sup><sup>1</sup> College of Mining and Coal, Inner Mongolia University of Science and Technology, Baotou 014010, China<sup>2</sup> Rizhao Riqing Technology Service Co., Ltd., Rizhao 276800, China<sup>3</sup> School of Civil Engineering, Inner Mongolia University of Science and Technology, Baotou 014010, China

\* Correspondence: zeyuduan0416@163.com; Tel.: +86-13347171676

**Abstract:** The mechanical properties of gas-containing coal and rock mass play important roles in controlling the occurrence and development of coal and gas outbursts. The gradual increase in mining depth will change the failure mechanism of gas-containing coal and rock mass. In order to further study the failure mechanism of gas-containing coal and rock mass, samples were taken from the gas-containing coal seam in the Wuhushan Coal Mine of the Wuhai Mining area of China. The mechanical parameters of coal samples during the failure process under different gas pressure conditions were measured and analyzed with the SAW-2000 rock mechanics testing machine, the gas-containing coal uniaxial compression device and inflation system. Meanwhile, the failure process and mechanical parameters of coal samples under different gas pressure were simulated by RFFPA<sup>2D</sup> gas plate numerical simulation software. The results show that with increasing gas pressure in the coal there is decrease in Compressive strength, Elastic modulus, Strain, Peak strength and Bearing capacity and increase in Poisson's ratio. When the failure state appears in the coal, the cracks are longer and wider, more random cracks are generated, and the damage degree of the coal is greater. The numerical analysis' results are in good agreement with experimental results. The research results are applicable to the gas bearing coal with the same or similar gas geological conditions. The tests can be carried out repeatedly and reasonable results can be obtained according to the physical and mechanical parameters of the actual coal seam and the occurrence of gas. On this basis, physical experiments and numerical simulations of triaxial compression can also be carried out to further study the mechanical characteristics of deformation and the failure of gas-containing coal under gas pressure and provide technical support for revealing the mechanism of coal and gas outbursts.



**Citation:** Liu, Y.; Xing, H.; Duan, Z.; Yu, C.; Tian, Z.; Teng, T. Study on Mechanical Characteristics of Deformation and the Failure of Gas-Containing Coal in the Wuhai Mining Area of China under Different Gas Pressure Conditions. *Appl. Sci.* **2022**, *12*, 10139. <https://doi.org/10.3390/app121910139>

Academic Editor: Stefano Invernizzi

Received: 13 August 2022

Accepted: 3 October 2022

Published: 9 October 2022

**Publisher's Note:** MDPI stays neutral with regard to jurisdictional claims in published maps and institutional affiliations.



**Copyright:** © 2022 by the authors. Licensee MDPI, Basel, Switzerland. This article is an open access article distributed under the terms and conditions of the Creative Commons Attribution (CC BY) license (<https://creativecommons.org/licenses/by/4.0/>).

**Keywords:** gas-containing coal; uniaxial compression; gas pressure; mechanical properties; damage

## 1. Introduction

The western region of China is rich in coal resources, which is the key development region of the country in the next 30–40 years. The main mining coal seam in this region is mainly distributed in 30~500 m. However, with the increasing depletion of shallow coal resources, the mining depth of coal resources in the western mining area is also increasing. Currently, there are many high gas mines in the western part of China, such as Wuhushan Coal Mine and Huangbaici Coal Mine in Wuhai Mining area of Inner Mongolia. With the increase in mining depth, the surrounding rock stress and gas pressure of coal mine will further increase, and coal and gas outbursts will become one of the main disasters threatening these mining areas [1].

The mechanical properties of coal and rock mass containing gas are important factors affecting the outburst of coal and gas. In view of the characteristics of deformation and mechanical response of gas-containing coal, scholars at home and abroad have conducted

substantial research and obtained certain research results. For example, Tankard [2], Bi-eniawaski [3], Atkinson [4], White [5], Karacan [6], and other scholars from Chongqing University [7–10], Henan Polytechnic University [11], China University of Mining and Technology [12,13], Northeastern University [14,15], Anhui University of Science and Technology [16], Qingdao University of Technology [17], China Coal Technology & Engineering Group [18], and other Chinese universities and research institutes carried out mechanical tests and CT scanning tests of gas-containing coal under different loading and unloading confined pressures and unloading axial pressure conditions using a conventional triaxial testing machine or true triaxial testing machine to study the factors affecting the mechanical properties of gas-containing coal. Scholars have also studied the deformation and failure characteristics of gas-containing coal and its constitutive model based on the catastrophe theory [19], chaotic object theory [20], elastic constitutive model of porous media [21,22], double media theory [23], coupled percolation, the splitting and damage model of rock fracture [24], creep model [25], Biot-type constitutive equation [26], HJC constitutive model [27], deformation and failure characteristics of gas-containing coal and its constitutive model. Some scholars further revealed the deformation and fracture laws of gas-containing coal and rock mass using numerical simulation methods and software such as the particle method [28], three-dimensional discrete fracture network modeling [29–31], remote sensing imagery [32], damage finite element Calculation program [33], COMSOL Multiphysics [34], and RPPA [35,36], et al. However, previous studies often combined several factors to comprehensively study the mechanism of coal and gas outbursts. There are relatively few in-depth research results on the mechanical properties and failure laws of gas-containing coal samples under different gas pressure conditions. There are also few research results on the mechanical characteristics of gas-containing coal in Wuhai mine area of Inner Mongolia. In this paper, the method of theoretical analysis, experimental testing and numerical simulation are combined used. Taking the gas-bearing coal seam in Wuhai Mining area of Inner Mongolia of China as the test base, the influence of different gas pressure on the mechanical characteristics of coal and rock mass containing gas and its deformation and fracture rule are analyzed emphatically. The research results have important theoretical significance and practical value for the prevention and control of coal and gas outburst accidents in Wuhai mining area and the drainage of coal seam gas under the influence of mining.

The test gas-containing coal samples in this paper were taken from the raw coal of No.9 coal seam of Wuhushan Coal Mine of Wuhai Mining area of China. Wuhushan Coal Mine is located in Wuda Mining area in the northern section of Helanshan coalfield of Inner Mongolia Autonomous Region of China. At present, the main coal seams are 9#, 10# and 12# coal seams which belong to the Upper Carboniferous Taiyuan Formation and the Lower Permian Shanxi Formation. The gas pressure of the main coal seam is between 0.5 Mpa to 2 Mpa, the porosity range is between 3.3% to 7.8%, and the coefficient of robustness is about 1.5. The roof and floor of coal seam are mainly shale, which has high stability and strength. The comprehensive mechanical mining method of striking long wall retreat is adopted, and the whole caving method is used to manage the roof in the coal mine. The absolute gas emission amount of Wuhushan Coal mine is 59.00 m<sup>3</sup>/min, and the relative gas emission amount is 18.87 m<sup>3</sup>/t. It is a high gas mine. The amount of gas emission in the mining face of the mine increases year by year, and the difficulty of gas disaster management is increased. Coupled with the influence of the overlying fire area, fault and other geological structures, the working face of Wuhushan Coal mine advances slowly, which seriously affects the mine safety production.

## **2. Analysis of Mechanical Characteristics and Influencing Factors of Deformation and Failure of Gas-Containing Coal**

### *2.1. Analysis of Gas Occurrence and Migration Law in Coal and Rock Mass*

As a type of porous medium, coal contains complex pore and fissure structures, which determine the occurrence characteristics of gas. The occurrence state of gas in coal is mainly

divided into the free state and adsorption state. The absorption state and water-soluble state of gas also exist, but the content is small. Gas migration can be divided into three processes: adsorption desorption, diffusion, and seepage. In the original coal, free gas and adsorbed gas will transformed into each other, and the quantity value between them is maintained within a certain range, which is in a dynamic equilibrium state of adsorption and desorption. In the process of coal mining, coal will be affected by external forces and deform. At this time, there will be a large number of cracks formed in the coal due to the failure of loads, leading to a continuous drop in gas pressure. When the gas pressure in the coal decreases to the critical desorption pressure, the internal gas will break away from the coal and transform into a free state. As a result, the amount of adsorbed gas gradually decrease, and the amount of free gas will gradually increase. This process will lead to a difference in gas pressure in the coal and the free surface's atmosphere pressure, resulting in gas pressure differences. Under the action of the pressure difference, the free gas percolates outward, and the gas content inside and outside the coal changes, resulting in a gas concentration difference. Due to the different internal and external concentration gradients, gas will flow from high to low concentrations, and this process is called diffusion motion. After that, the migration form of gas in coal fissures becomes seepage state, which follows Darcy's law.

## 2.2. Analysis of Influencing Factors on Mechanical Characteristics of Gas-Containing Coal

### (1) Effect of confining pressure on mechanical properties of gas-containing coal

Relevant scholars [37] have made linear fittings between compressive strength and the confining pressure of gas-containing coal under different confining pressure conditions, and they observed that there is an obvious linear relationship between compressive strength and confining pressure. With an increase in confining pressure, the compressive strength of gas-containing coal increases gradually, and its bearing capacity also increases continuously.

### (2) The effect of porosity on mechanical properties of gas-containing coal

The macroscopic method is usually adopted to describe the porosity of gas-containing coal, which is defined as the percentage of the pore volume in the material to the total volume of the material in the natural state:

$$n = \frac{v_p}{v} \times 100\% = \frac{v - v_s}{v} \times 100\% \quad (1)$$

where  $n$  is the porosity of the gas-containing coal, which is dimensionless;  $v_p$  is the volume occupied by pores and cracks in gas-containing coal;  $v_s$  is the solid volume of gas-containing coal.

According to the above equation, when the porosity of coal changes, the volume deformation of coal will be caused, and the larger the porosity, the more obvious the deformation of gas-containing coal [38].

### (3) Influence of seepage on mechanical properties of gas-containing coal

According to the basic theory of coal and rock mass deformation and gas seepage, coupled with the interaction between gas and deformation of coal, a mathematical equation of gas-solid coupling in the fracture process of gas-containing coal can be established [39].

Consistent with the linear permeation law, the gas motion equation is established as follows:

$$q_i = -\lambda_{ij} \frac{dP}{dn} \quad (2)$$

where  $q_i$  is the gas seepage velocity component ( $i = 1, 2, 3 \dots$ ) (m/d);  $\lambda_{ij}$  is the component of the permeability coefficient tensor ( $i, j = 1, 2, 3, \dots$ ) ( $\text{m}^2/(\text{MPa}^2 \cdot \text{d})$ );  $P$  is the square of the coal seam's gas pressure ( $\text{MPa}^2$ ).

According to the gas content coefficient method, the gas content equation can be expressed as follows:

$$X = A\sqrt{p} \quad (3)$$

where  $X$  is the gas content in coal rock ( $\text{m}^3/\text{t}$ );  $A$  is the gas content coefficient of coal seam ( $\text{m}^3/(\text{m}^3 \cdot \text{MPa}^{1/2})$ );  $P$  is coal seam gas pressure (MPa).

At the same time, seepage tests under triaxial compression show the following [40]: There is a negative exponential relationship between the effective volumetric stress and permeability before the peak point of gas-containing coal samples. After the peak point, there is still an exponential relationship between effective volumetric stress and permeability, but the coefficient changes, which is different from that before the peak point. The permeability of coal samples containing gas changes in the opposite direction to the effective volumetric stress, that is, when the effective volumetric stress increases, permeability decreases, and vice versa.

#### (4) Effect of gas pressure on mechanical properties of gas-containing coal

Under the condition of certain axial and confining pressures, the increase in gas pressure has two effects on outburst coal samples: one is that its mechanical effect leads to the increase in coal pores; the other is that its adsorption effect leads to a decrease in coal pores. There is a critical gas pressure that is less than the critical gas pressure range, and an increase in gas pressure caused by pore expansions is smaller than the adsorption of gas caused by pore contraction, resulting in a reduction in permeable pores and gas permeability and a decrease in the permeability coefficient. When the pore gas exceeds this critical gas pressure, the expansion of pores caused by the increase in gas pressure is greater than the contraction of pores caused by the adsorption of gas, which leads to an increase in permeable pores and the increase in gas permeability and the permeability coefficient of coal samples [41,42].

### 3. Uniaxial Compression Experimental Study on Deformation and Failure Mechanical Properties of Gas-Containing Coal under Different Gas Pressure Conditions

#### 3.1. Preparation Method of Coal Sample Containing Gas

##### (1) Coal sample preparation

The raw coal sample was broken apart by placing it into a pulverizer, and then a vibrating screen diagram was used to screen the pulverized coal particles of different sizes. The binder used in the experiment was a mixture of tap water and sodium humate [43], with a concentration of 15%. The binder and pulverized coal are mixed evenly and then loaded into the customized briquette mold in Figure 1a. Some briquette samples are shown in Figure 1b.

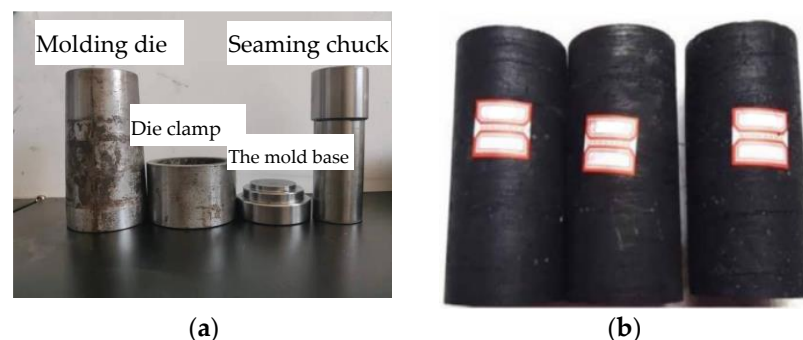


**Figure 1.** Briquette mold and briquette sample: (a) coal mold; (b) partial briquette coal sample.

##### (2) Test equipment

The SAW-2000 rock mechanics testing machine was used as the carrier, and the mechanical parameters of coal samples under loading failure process under different gas pressures were measured and analyzed in combination with the uniaxial compression device and the inflation system. The entire test system is shown in Figure 2.

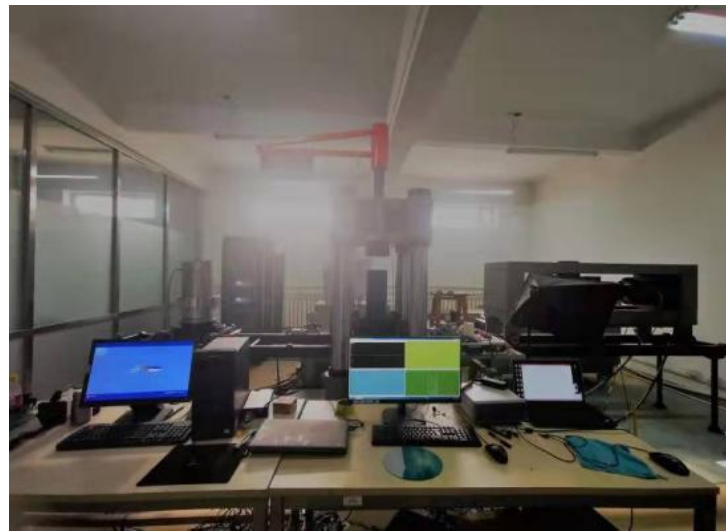


**Figure 2.** Uniaxial compression test system.

### 3.2. Uniaxial Compression Test Process of Gas-Containing Coal

#### 3.2.1. Test Plan

In order to study the influence of different gas pressures on the uniaxial compression failure law of gas-containing coal, the uniaxial compression test scheme of gas-containing coal is formulated, which is detailed in Table 1.

**Table 1.** Uniaxial compression test scheme of gas-containing coal.

Test Plan	Gas Pressure/MPa	Loading Rate/mm/min	Water/Cement Ratio/g/g	Briquette Forming Pressure/MPa
The first group	0	0.02	9.5:0.5	15
The second group	1	0.02	9.5:0.5	15
The third group	2	0.02	9.5:0.5	15

#### 3.2.2. Test Steps

- (1) The standard coal samples prepared from the Wuhushan Coal Mine in Wuhai Mining area, and they were divided into three groups and numbered; the original physical parameters of each group were recorded.
- (2) The first group of coal samples was numbered as A1–1, A1–2, and A1–3, which are subjected to conventional uniaxial compression tests.
- (3) The second group of coal samples were numbered as A2–1, A2–2 and A2–3. Uniaxial compression test was carried out on this group of coal samples under the gas pressure of 1 MPa.
- (4) The third group of coal samples was numbered A3–1, A3–2, and A3–3. A uniaxial compression test is carried out on this group of coal samples under the gas pressure of 2 MPa, and the process is the same as that of the second group of coal samples.
- (5) Experimentalists compared and analyzed the three groups of test data and summarized the rules.

### 3.3. Influence Analysis of Different Gas Pressure on Mechanical Properties of Coal Samples Containing Gas

- (1) Stress–strain curve analysis of coal samples

The stress–strain curves of coal samples under different gas pressures are shown in Figure 3. The stress–strain curve of gas-containing coal does not change obviously in the initial compaction stage. With the continuous increase in the load on the coal sample, the gas-containing coal begins to fail and enters the elastic deformation stage, and the

stress–strain in the elastic deformation stage shows obvious linear characteristics. As the load continues to increase, the cracks in the coal develop rapidly and form cracks, which is the stage of plastic deformation. The strain and peak strength of gas-containing coals near the final rupture decrease with the increase in gas pressure. It can be seen that the increase in gas pressure under conventional uniaxial loading can weaken the bearing capacity of gas-containing coal.

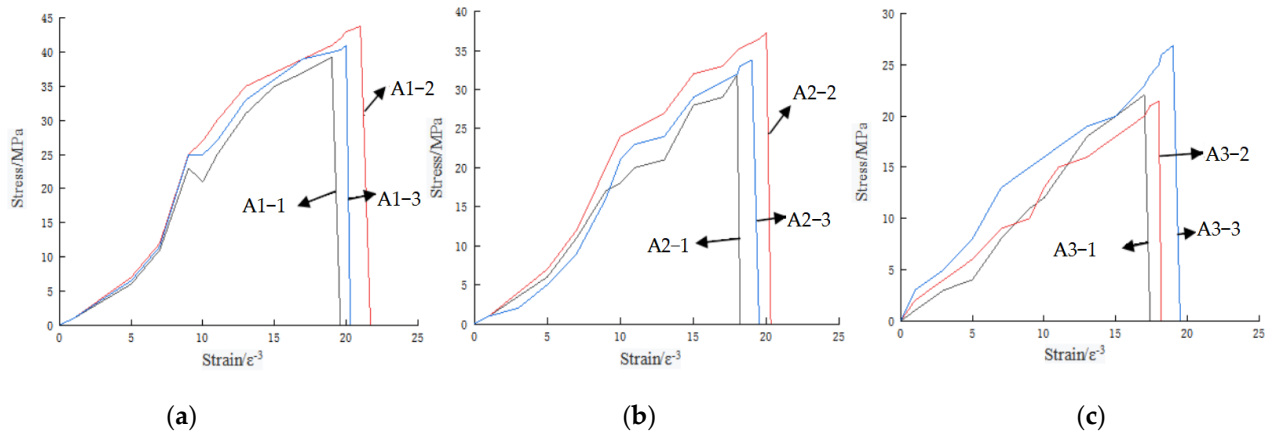


**Figure 3.** Full stress–strain curve of coal sample under different gas pressure. (a) The gas pressure is 0 MPa; (b) the gas pressure is 1 MPa; (c) the gas pressure is 2 MPa.

(2) Analysis of mechanical parameters of coal samples

Experimental results of the mechanical properties of coal samples containing gas under different gas pressures are shown in Table 2. The relationship between the compressive strength, elastic modulus, and Poisson’s ratio of coal samples and gas pressure under different gas pressure can be obtained by analysis.

**Table 2.** Test results of mechanical properties of coal samples under different gas pressures.

Gas Pressure/MPa	Coal Sample Number	The Compressive Strength/MPa	Modulus of Elasticity/GPa	Poisson’s Ratio
0	A1-1	39.27	2.249	0.233
	A1-2	43.83	2.327	0.267
	A1-3	40.45	2.286	0.246
On average		41.18	2.29	0.25
1	A2-1	31.879	1.526	0.288
	A2-2	37.236	1.998	0.242
	A2-3	33.754	1.529	0.259
On average		34.29	1.68	0.263
2	A3-1	22.072	1.63	0.324
	A3-2	21.478	1.14	0.261
	A3-3	26.873	1.03	0.282
On average		23.47	1.27	0.29

The mechanical properties of the test results of coal samples containing gas under different gas pressures were fitted to the data, and the following fitting formulas were obtained.

The relationship between compressive strength and gas pressure is as follows:

$$y_1 = 41.835 - 8.855x \quad (4)$$

where  $y_1$  is the compressive strength (MPa), and  $x$  is Gas pressure (MPa).

The relationship between elastic modulus and gas pressure is as follows:

$$y_2 = 2.257 - 0.51x \quad (5)$$

where  $y_2$  is Modulus of elasticity (GPa), and  $x$  is Gas pressure (MPa).

The relationship between Poisson's ratio and gas pressure is as follows:

$$y_3 = 0.24767 + 0.02x \quad (6)$$

where  $y_3$  is Poisson's ratio, and  $x$  is Gas pressure (MPa).

The mechanical property data of coal samples under different gas pressures were drawn in a scatter plot, and a fitting curve was obtained, as shown in Figure 4. The correlation coefficients of compressive strength, elastic modulus, and Poisson's ratio with gas pressures are 0.968, 0.975, and 0.92, respectively, indicating that there is a good linear relationship between the mechanical properties of coal samples and gas pressure.

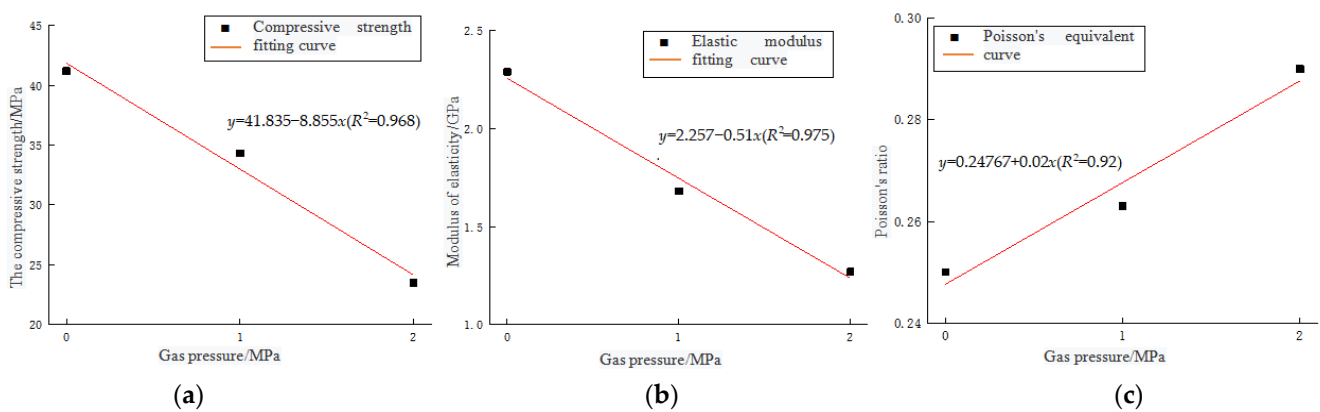


**Figure 4.** Fitting curves of the mechanical properties of coal samples under different gas pressures. (a) Compressive strength and gas pressure; (b) elastic modulus and gas pressure; (c) Poisson's ratio and gas pressure.

#### 4. Numerical Simulation of Mechanical Characteristics of Failure, Deformation and Failure of Gas-Containing Coal under Different Gas Pressure Conditions

In this paper, the numerical simulation of failure, deformation and mechanical characteristics of gas-containing coal under different gas pressure conditions was carried out by using RFPA<sup>2D</sup> gas plate software (gas coal rock fracture process analysis system). The RFPA<sup>2D</sup> gas plate software is mainly used in the numerical tests of basic mechanical properties and basic seepage properties during the fracture process of gas-containing coal and rock. The numerical results can visually and graphically show the evolution characteristics of stress field and gas flow field during the fracture process of gas-containing coal and rock.

##### 4.1. Determination of Numerical Model and Simulation Parameters for Coal Samples Containing Gas

###### (1) Mathematical model of failure, deformation, and the failure of gas-containing coal

In the RFPA<sup>2D</sup> gas plate software, assuming that the failure and deformation failure of gas-containing coal is the test of monomer coal, the permeability-damage coupling equation [39] can be adopted, and the elastic modulus of the damage element can be expressed as follows

$$E = (1 - D)E_0 \quad (7)$$

where  $E$  is the elastic modulus of the damaged element;  $E_0$  is the elastic modulus of the element without damage;  $D$  is the damage variable. In addition, these parameters are assumed scalars.

The Moore-Coulomb criterion is adopted for the coal failure criterion, i.e.,

$$\sigma_1 - \sigma_3 \frac{1 + \sin \phi}{1 - \sin \phi} \geq f_c \tag{8}$$

where  $\sigma_1$  is the maximum principal stress;  $\sigma_3$  is the minimum principal stress;  $\phi$  is the Angle of internal friction;  $f_c$  is uniaxial compressive strength.

When the shear stress reaches the more-Coulomb loss threshold, the damage variable  $D$  is expressed as follows

$$D = \begin{cases} 0, & \varepsilon < \varepsilon_{c0} \\ 1 - \frac{f_{cr}}{E_0 \varepsilon}, & \varepsilon_{c0} \leq \varepsilon \end{cases} \tag{9}$$

where  $f_{cr}$  is the residual compressive strength;  $\varepsilon$  is the dependent variable;  $\varepsilon_{c0}$  is the maximum compressive strain.

Damage will cause the gas permeability coefficient of coal material to increase sharply, that is, the change of the gas permeability coefficient can be described as follows

$$\lambda = \begin{cases} \lambda_0 e^{-\beta(\sigma_1 - \alpha p)}, & D = 0 \\ \xi \lambda_0 e^{-\beta(\sigma_1 - \alpha p)}, & D > 0 \end{cases} \tag{10}$$

where  $\lambda$  is the air permeability coefficient;  $\lambda_0$  is the initial air permeability coefficient;  $\xi$  is the increasing rate of permeability coefficient;  $\alpha$  is gas pressure coefficient;  $\beta$  is permeability coupling coefficient.

(2) Establishment of numerical model for deformation and failure of gas-containing coal

The stress-strain characteristics and mechanical parameters of coal samples under different gas pressures in the process of loading failure were studied by using the RFPA<sup>2D</sup> numerical simulation software. The main variable controlled by numerical simulation was gas pressure, and the model of coal samples containing gas was established, as shown in Figure 5.

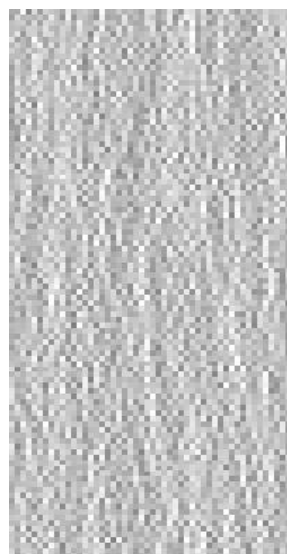


Figure 5. Initial model of coal sample containing gas.

(3) The numerical simulation process, initial and boundary conditions of deformation, and failure of gas-containing coal

The problem analysis process of RFPA<sup>2D</sup> gas plate software is shown in Figure 6.

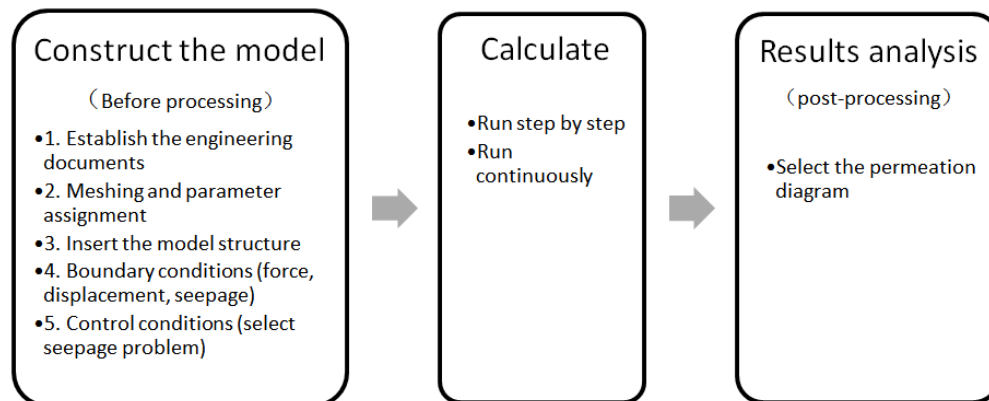


Figure 6. Problem analysis process of RFPA<sup>2D</sup> gas plate software.

The numerical simulation process, initial and boundary conditions of deformation, and failure of gas-containing coal are set according to the following methods [44–47].

A physical model of gas-containing coal samples was established, the size of which was 50 mm × 100 mm. The grid was divided into 90 × 180, the elastic modulus was set as 10,000 MPa, the strength was set as 100 MPa, the Poisson’s ratio was set as 0.25, the pressure ratio was set as 10, and the internal friction angle was set as 30. The horizontal and vertical permeability coefficients of the model were set as 0.1, the gas content coefficient was set as 3, the gas pressure coefficient was set as 1, the coupling coefficient was set as 0.2, and pore pressure coefficients were set as 0, 0.5, 1, 1.5, and 2. The loading process of the model specimen was displacement loading in the Y direction and free constraint in the X direction, and the loading rate was 0.005 mm/s. The loading steps of the model were set to 100. The StepInStep option, confined water option, and dynamic problem option were selected. The seepage time was set to 24 h, and the osmotic pressure value was set to 2 MPa. The Shear and AE option was selected in the Custom Options Settings. The gas pressure option was selected and the gas pressure in the model is the same as the osmotic pressure on the left and right sides of the model, and the flow on the upper and lower sides was 0.

#### 4.2. Analysis of Numerical Simulation Results of Deformation and Failure Mechanical Characteristics of Gas-Containing Coal under Different Gas Pressure Conditions

##### 4.2.1. Analysis of Simulation Results of the Influence of Different Gas Pressure on Mechanical Parameters of Coal Samples Containing Gas

By conducting the numerical simulation test of the uniaxial compression of coal samples under different gas pressures, the stress–strain curve of the uniaxial compression of coal samples containing gas under different gas pressures is obtained, as shown in Figure 7.

Meanwhile, the relationship between the loading force (compressive strength) and elastic modulus of coal samples can be further analyzed according to the numerical simulation results, as shown in Table 3.

Table 3. Table of relation between different gas pressure and mechanical properties of coal samples.

Gas Pressure/MPa	Loading Force/N	Modulus of Elasticity/GPa
0	792.1	10.963
0.5	723.4	10.673
1	672.2	9.857
1.5	593.7	9.163
2	565.5	8.865

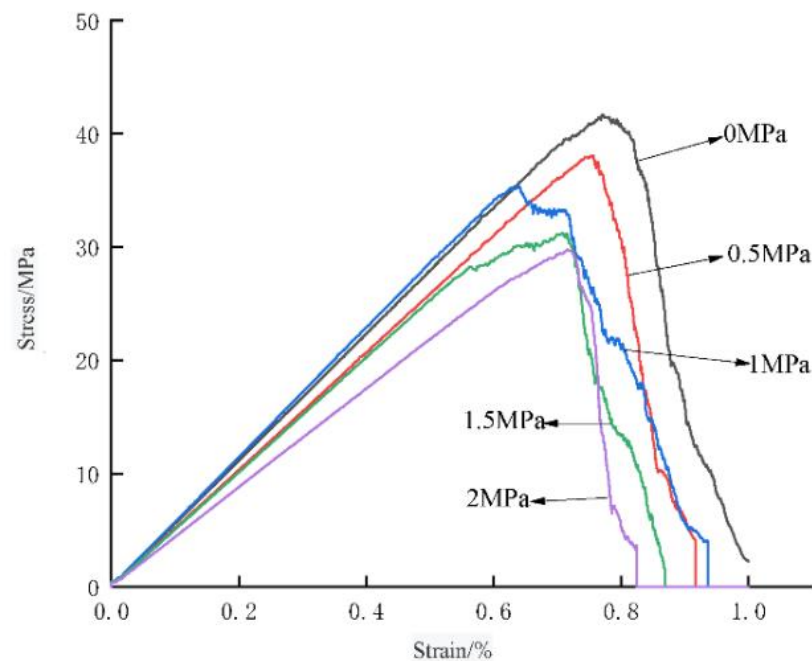


**Figure 7.** Stress and strain curves of coal samples under uniaxial compression with different gas pressures.

It can be seen from Table 3 that with the increase in gas pressure, the loading force (compressive strength) of the coal sample decreases from 792.1 N to 565.5 N, and its compressive strength decreases by 28.61%. The loading force (compressive strength) of the coal sample is negatively correlated with gas pressure, and the greater the gas pressure, the smaller the loading force required for the coal sample to reach peak failure. With the increase in gas pressure, the elastic modulus of the coal sample decreases from 10.963 MPa to 8.865 MPa, and its elastic modulus decreases by 19.14%. There is a negative correlation between the elastic modulus of coal sample and gas pressure, and the greater the gas pressure, the smaller the elastic modulus of coal sample. This is consistent with the test's results.

#### 4.2.2. Analysis of Simulation Results of Fracture Process of Gas-Containing Coal under Different Gas Pressure Conditions

##### (1) Fracture analysis of coal samples when the gas pressure is 0 MPa

The deformation and rupture of coal samples when the gas pressure is 0 MPa is shown in Figure 8. When the loading step is 35, the failure points are few, the failure of a single element has little influence on the surrounding elements, and the correlation scale between micro-fractures is relatively limited. When the loading step is 50, the failure points of the coal sample increase, and the failure points are randomly distributed in the coal sample. When the loading step is 68, the internal structure of the coal sample changes significantly, and the crack develops from the lower edge of the coal sample to the upper right, and the crack expands through to form a macroscopic main crack.

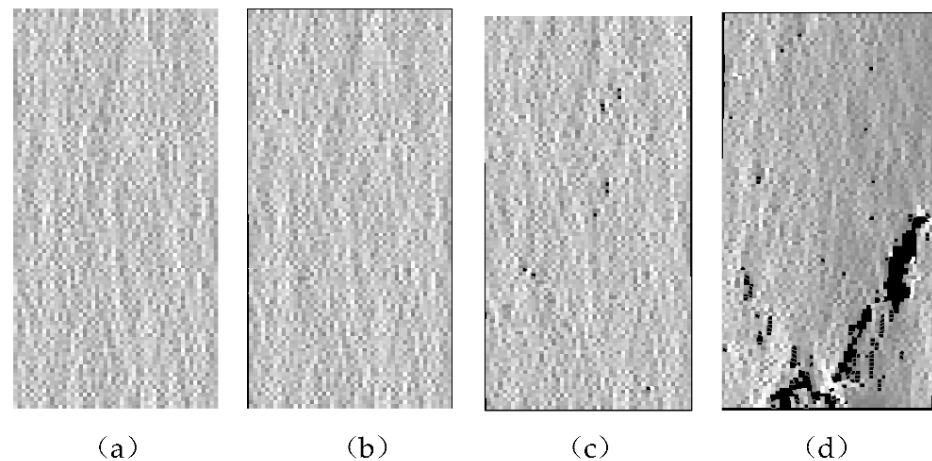


**Figure 8.** Deformation and rupture of coal samples when the gas pressure is 0 MPa: (a) the loading step is 15; (b) the loading step is 35; (c) the loading step is 50; (d) the loading step is 68.

(2) Fracture analysis of coal samples when the gas pressure is 0.5 MPa

The deformation and rupture of coal samples when the gas pressure is 0.5 MPa are shown in Figure 9. When the loading step is 28, the failure points number a few, the failure of a single element has little influence on the surrounding elements, and the correlation scale between micro-fractures is relatively limited. When the loading step is 49, the failure points of the coal sample increase, and the failure points are randomly distributed in the coal sample. When the loading step is 65, the internal structure of the coal sample changes significantly, and the crack develops from the upper edge of the coal sample to the lower right; the crack expands to form a macroscopic main crack.

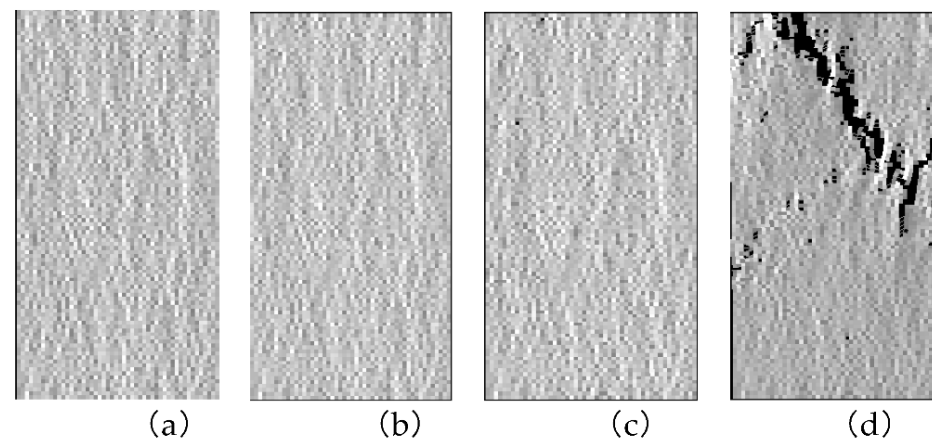


**Figure 9.** Deformation and rupture of coal samples when the gas pressure is 0.5 MPa: (a) the loading step is 17; (b) the loading step is 28; (c) the loading step is 49; (d) the loading step is 65.

(3) Fracture analysis of coal samples when the gas pressure is 1 MPa

The deformation and rupture of coal samples when the gas pressure is 1 MPa are shown in Figure 10. When the loading step is 29, there are fewer failure points. The failure of a single unit has little influence on its surrounding units, and the correlation scale between micro-fractures is relatively limited. When the loading step is 41, the failure points of the coal sample increase, and the failure points are randomly distributed in the coal sample. When the loading step is 63, the internal structure of the coal sample changes significantly, and the crack develops from the upper edge of the coal sample to the middle part, and a macroscopic main crack is formed through the expansion of the crack.

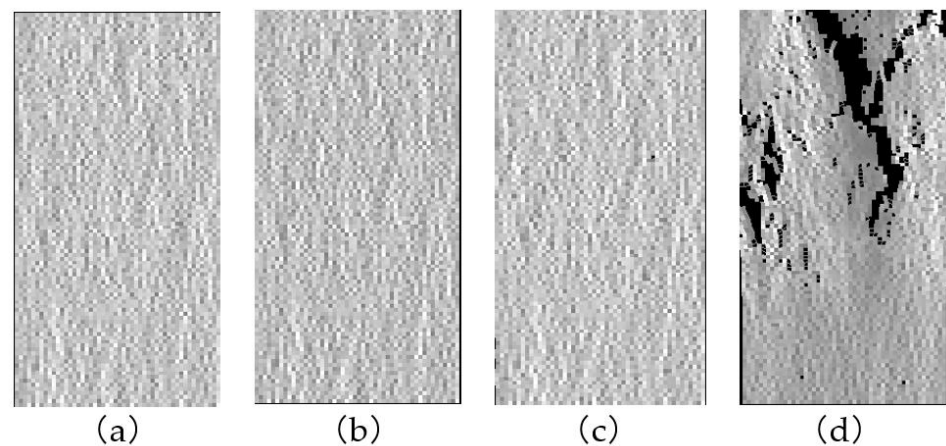


**Figure 10.** Deformation and rupture of coal samples when the gas pressure is 1 MPa: (a) the loading step is 16; (b) the loading step is 29; (c) the loading step is 41; (d) the loading step is 63.

(4) Fracture analysis of coal samples when the gas pressure is 1.5 MPa

The deformation and rupture of coal samples when the gas pressure is 1.5 MPa are shown in Figure 11. When the loading step is 33, the failure points number a few, the failure of a single element has little influence on the surrounding elements, and the correlation scale between micro-fractures is relatively limited. When the loading step is 47, the failure points of the coal sample increase, and the failure points are randomly distributed in the coal sample. When the loading step is 60, the internal structure of the coal sample changes significantly, and the crack develops from the lower edge of the coal sample to the middle part; the crack expands to form a macroscopic main crack.

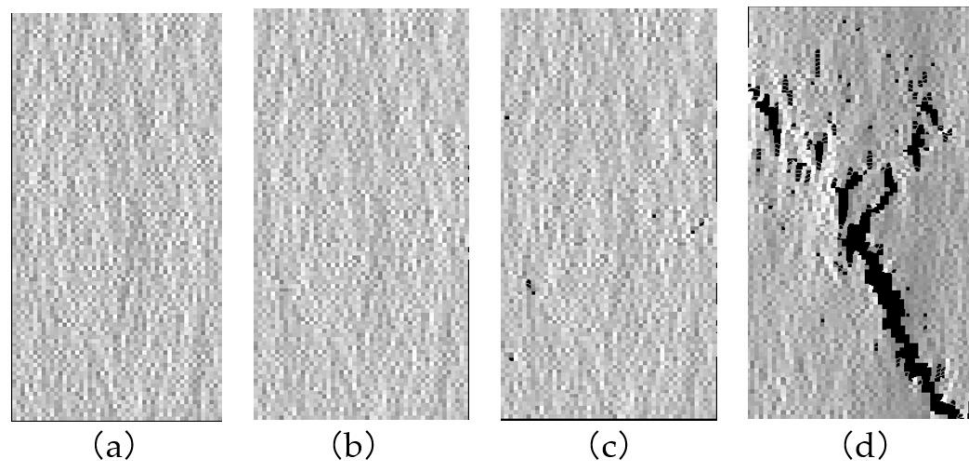


**Figure 11.** Deformation and rupture of coal samples when the gas pressure is 1.5MPa: (a) the loading step is 15; (b) the loading step is 33; (c) the loading step is 47; (d) the loading step is 60.

(5) Fracture analysis of coal samples when the gas pressure is 2 MPa

The deformation and rupture of coal samples when the gas pressure is 2 MPa are shown in Figure 12. When the loading step is 36, the failure points number a few, the failure of a single element has little influence on the surrounding elements, and the correlation scale between micro-fractures is relatively limited. When the loading step is 50, the failure points of the coal sample increase, and the failure points are randomly distributed in the coal sample. When the loading step is 58, the internal structure of the coal sample changes significantly, and the crack develops from the upper edge of the coal sample to the middle part; the crack expands to form a macroscopic main crack.

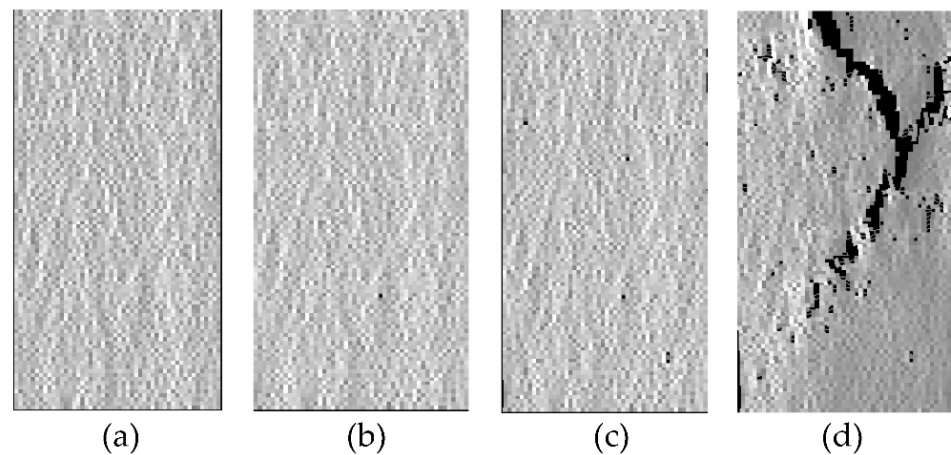


**Figure 12.** Deformation and rupture of coal samples when the gas pressure is 2 MPa: (a) the loading step is 17; (b) the loading step is 36; (c) the loading step is 50; (d) the loading step is 58.

(6) Analysis and comparison of coal sample rupture under different gas pressure conditions

The deformation and rupture of coal samples under different gas pressure conditions are shown in Figure 13. By comparison, it was found that with the increase in gas pressure, the crack of coal sample grows longer when it reaches the final failure state. As observed in Figure 13e, when the gas pressure is 2 MPa, the crack almost runs through the entire coal sample. With the increase in gas pressure, the crack of coal sample widens. As observed from Figure 13, with the increase in gas pressure, the loading steps used for coal samples to reach the final failure state gradually decrease, which indicates that with the increase in gas pressure, the rupture speed of the coal sample after loading is accelerated, the time to reach the final failure state is shortened, and the bearing capacity of coal sample is weakened. This is consistent with the results of theoretical analysis and test.

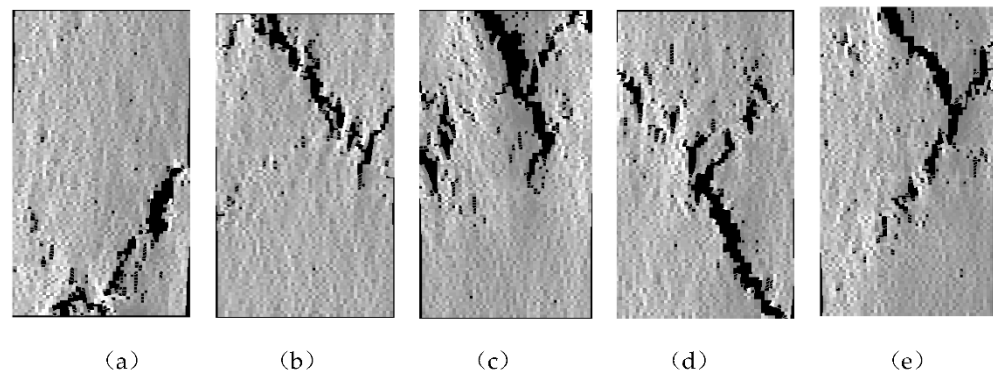


**Figure 13.** Deformation and rupture of coal samples under different gas pressure conditions: (a) the gas pressure is 0 MPa and the loading step is 68; (b) the gas pressure is 0.5 MPa and the loading step is 65; (c) the gas pressure is 1 MPa and the loading step is 63; (d) the gas pressure is 1.5 MPa and the loading step is 60; (e) the gas pressure is 2 MPa and the loading step is 58.

## 5. Conclusions and Discussion

- (1) The experimental and numerical simulation results show that with increasing gas pressure in the coal, there is decrease in Compressive strength, Elastic modulus, Strain, Peak strength and Bearing capacity and increase in Poisson's ratio. When the failure state appears in the coal, the cracks are longer and wider, more random cracks are generated, and the damage degree of the coal is greater.
- (2) The physical test method of uniaxial compression and the modeling method and procedure of numerical test of deformation and failure of gas-containing coal are

applicable to the gas-containing coal with the same or similar gas geological conditions. According to the physical and mechanical parameters of the actual coal seam (such as elastic modulus, compressive strength, Poisson's ratio, internal friction angle, etc.) and the gas occurrence, by adjusting gas pressure, seepage pressure, porosity, permeability coefficient and other parameters, this kind of test can be repeated and reasonable test results will be obtained.

- (3) Due to the cost and time of the test, only uniaxial compression physical test of deformation and failure of gas-containing coal under different gas pressure conditions is carried out in the paper. The corresponding triaxial compression physical test will be carried out in the later stage, so as to provide more reliable data support for the study of deformation and failure law of gas-containing coal.

**Author Contributions:** The preparation of the initial and revised version of the manuscript and figures was performed by Y.L., H.X. and Z.D.; T.T., C.Y. and Z.T. are responsible for providing theoretical guidance and article revision. All authors have read and agreed to the published version of the manuscript.

**Funding:** This work was financially supported by the National Natural Science Foundation of China (No. 51427804) and Inner Mongolia Natural Science Foundation Project (No. 2021MS05059, 2020MS05041).

**Data Availability Statement:** The original contributions presented in the study are included in the article; further inquiries can be directed to the corresponding author.

**Conflicts of Interest:** The authors declare no conflict of interest.

## References

- Liu, Y.J.; Yuan, L.; Xue, J.H.; Tian, J.C.; Duan, C.R.; Chen, B.L. Research status and development trend of mechanism and simulation test of coal and gas outburst. *J. Mine Autom.* **2018**, *44*, 43–50. [[CrossRef](#)]
- Tankard, H.G. The Effect of Sorbed Carbon Dioxide Upon the Strength of Coals. Ph.D. Thesis, University of Sydney, Sydney, Australia, 1957; pp. 5–10.
- Bieniawski, Z.T. The effect of specimen size on compression strength in coal. *Int. J. Rock Mech. Min. Sci.* **1968**, *5*, 325–333. [[CrossRef](#)]
- Atkinson, R.H.; Yim, K.H. Strength characteristics of US coal. *Proc. 18th. Symp. Rock Mech. Colo. Sch. Mines Press Gold.* **1977**, *2*, 1–3.
- White, J.M. Mode of deformation of Rosebud coal. *Int. J. Rock Mech. Min. Sci. Geomech. Abstr.* **1980**, *17*, 129–130. [[CrossRef](#)]
- Karacan, C.Ö. Swelling-induced volumetric strains internal to a stressed coal associated with CO<sub>2</sub> sorption. *Int. J. Coal Geol.* **2007**, *72*, 209–220. [[CrossRef](#)]
- Yin, G.Z.; Huang, Q.X.; Zhang, D.M.; Wang, D.K. Test study of gas seepage characteristics of gas-containing coal specimen during process of deformation and failure in geostress field. *Chin. J. Rock Mech. Eng.* **2010**, *29*, 336–343.
- Zhao, H.B.; Zhang, H.B.; Yin, G.Z. Experiments on triaxial mechanical properties of soft gas-containing coal. *J. Chongqing Univ.* **2013**, *36*, 103–109.
- Yuan, M.; Xu, J.; Li, B.; Wang, Z.; Du, Y.Q.; Xu, S.Q. Experimental study on influence of particle size on mechanical properties and permeability of briquette coal containing gas. *Saf. Coal Mines* **2016**, *47*, 24–28.
- Liao, X.J.; Jiang, C.B.; Duan, M.K.; Tian, W.J. Influence of temperature on the mechanical and deformation properties of containing-gas raw coal under mining. *J. Northeast. Univ. Nat. Sci.* **2017**, *38*, 1347–1355.
- Wang, D.K.; Zhang, H.; Wei, J.P.; Wu, Y.; Zhang, H.T.; Yao, B.H.; Fu, J.H.; Zhao, L.Z. Dynamic evolution characteristics of fractures in gas-containing coal under the influence of gas pressure using industrial CT scanning technology. *J. China Coal Soc.* **2021**, *46*, 3550–3564. [[CrossRef](#)]
- Xin, C.P.; Zhang, X.; Du, F.; Liu, Y.L. Experimental study on influence of piecewise variable speed loading on mechanical properties of outburst coal containing gas. *J. Saf. Sci. Technol.* **2018**, *14*, 133–139.
- Niu, Y.X. Study on Mechanical Behavior and Energy Evolution Characteristics of Gas-Solid Coupling Containing Gas under Triaxial Compression. Master's Thesis, China University of Mining and Technology, Xuzhou, China, 2021.
- Li, J.T.; Liang, W.X.; He, Z.H. Quantitative characterization of micro-structure of gas-bearing coal in Tunlan mining. *J. Northeast. Univ. Nat. Sci.* **2019**, *40*, 886–890.
- Tian, Z.C.; Tang, C.A.; Liu, Y.J.; Tang, Y.B. Zonal disintegration test of deep tunnel under plane strain conditions. *Int. J. Coal Sci. Technol.* **2020**, *7*, 337–349. [[CrossRef](#)]
- Liu, H.F. Study on Mechanical Characteristics of Gas-Containing Coal under Different Loading Rates. Master's Thesis, Anhui University of Science and Technology, Huainan, China, 2018.
- Zhang, R. Study on Mechanical Properties and Failure Precursor Characteristics of Gas-Containing Coal Subjected to True Triaxial Loading-Unloading. Master's Thesis, Qingdao University of Technology, Qingdao, China, 2021.

18. Liu, K.D. Mechanical properties of ram coal containing gas under high triaxial stress compression. *Chin. J. Rock Mech. Eng.* **2017**, *36*, 380–393. [[CrossRef](#)]
19. Yin, G.Z.; Li, H.; Xian, X.F.; Feng, T. The catastrophic theory model of instability of coal and rock mass. *J. Chongqing Univ. Nat. Sci.* **1994**, *01*, 23–28.
20. Jiang, Y.D.; Zhu, J.; Zhao, Y.X.; Liu, J.H.; Wang, H.W. Constitutive equations of coal containing methane based on mixture. *J. China Coal Soc.* **2007**, *11*, 1132–1137.
21. Connell, L.D.; Lu, M.; Pan, Z. An analytical coal permeability model for tri-axial strain and stress conditions. *Int. J. Coal Geol.* **2010**, *84*, 103–114. [[CrossRef](#)]
22. Wang, J.G.; Kabir, A.; Liu, J.; Chen, Z.W. Effects of non-Darcy flow on the performance of coal seam gas wells. *Int. J. Coal Geol.* **2012**, *93*, 62–74. [[CrossRef](#)]
23. Zhang, J.X. Research on Dynamic Coupling Model and Its Application Base on the Pore-Fracture Dual Media Characteristics of Gas-Containing Coal. Master's Thesis, Henan Polytechnic University, Jiaozuo, China, 2016.
24. Zhao, Y.L.; Cao, P.; Ma, W.H.; Tang, J.Z.; Wang, W.; Wang, W.J. Coupling model of seepage-splitting-damage of rock mass fractures and its application. *J. Cent. South Univ. Sci. Technol.* **2017**, *48*, 794–803.
25. Li, X.C.; Zhang, L.; Li, Z.B.; Jiang, Y.; Nie, B.S.; Zhao, Y.L.; Yang, C.L. Creep law and model of coal under triaxial loading at different gas pressures. *J. China Coal Soc.* **2018**, *43*, 473–482. [[CrossRef](#)]
26. Wu, G.S.; Yu, W.J.; Wang, P.; Liu, Z.; Liu, F.F.; Huang, Z. Deformation failure mechanism and experimental study of gas-containing coal rock mass based on percolation mechanism. *J. China Coal Soc.* **2018**, *43*, 724–734. [[CrossRef](#)]
27. Xie, B.J.; Zhao, Z.M.; Xu, X.M.; Zhao, Y.C. HJC constitutive model and numerical simulation of hammer damage with gas-containing coal. *J. China Coal Soc.* **2018**, *43*, 2789–2799. [[CrossRef](#)]
28. Huang, W.X.; Liu, D.W.; Xia, M. Study of meso-mechanism of coal and gas outburst. *Chin. J. Rock Mech. Eng.* **2017**, *36*, 429–436. [[CrossRef](#)]
29. Azarafza, M.; Akgün, H.; Asghari-Kaljahi, E. Stochastic geometry model of rock mass fracture network in tunnels. *Q. J. Eng. Geol. Hydrogeol.* **2018**, *51*, 379–386. [[CrossRef](#)]
30. Huang, N.; Liu, R.C.; Jiang, Y.Y.; Cheng, Y.F. Development and application of three-dimensional discrete fracture network modeling approach for fluid flow in fractured rock masses. *J. Nat. Gas Sci. Eng.* **2021**, *91*, 103957. [[CrossRef](#)]
31. Wu, N.; Liang, Z.Z.; Zhang, Z.H.; Li, S.H.; Lang, Y.X. Development and verification of three-dimensional equivalent discrete fracture network modelling based on the finite element method. *Eng. Geol.* **2022**, *306*, 106759. [[CrossRef](#)]
32. Mehrabi, A.; Derakhshani, R.; Nilfouroushan, F.; Rahnamarad, J.; Azarafza, M. Spatiotemporal subsidence over Pabdana coal mine Kerman Province, central Iran using time-series of Sentinel-1 remote sensing imagery. *Epis. J. Int. Geosci.* **2022**. [[CrossRef](#)]
33. Liu, X.G. Study on the Deformation and Failure Characteristics and the Permeation Behavior of Gas-Saturated Coal. Ph.D. Thesis, China University of Mining and Technology, Xuzhou, China, 2013.
34. Huang, X.C. Study and application on thermo-gas-mechanical coupling model of gas-containing coal. *Coal Sci. Technol.* **2018**, *46*, 146–152 + 175.
35. Zhang, Y. Stress and Gas Pressure of Coal and Rock Containing Gas Numerical Simulation of Coupled Characteristics. Master's Thesis, Anhui University of Science and Technology, Huainan, China, 2019.
36. Xu, T.; Tang, C.A.; Song, L.; Yang, T.H.; Liang, Z.Z. Numerical simulation of coupled gas flow in failure process of gassy coal-rock. *Chin. J. Rock Mech. Eng.* **2005**, *10*, 1667–1673.
37. Jia, H.Y.; Wang, K.; Wang, Y.B.; Sun, X.K. Permeability characteristics of gas-bearing coal specimens under cyclic loading-unloading of confining. *J. China Coal Soc.* **2020**, *45*, 1710–1718.
38. Liu, Y.J.; Xing, H.; Li, M.; Cui, Y.N.; Teng, T. Failure mechanism and numerical analysis of gas-containing coal with different porosity. *Min. Technol.* **2022**, *22*, 41–44.
39. Yuan, L.; Liu, Y.J.; Tian, Z.C.; Tuan, C.A.; Xue, J.H.; Duan, C.R.; Zhang, H. Numerical test and application of gas pre-drainage in an extra-thick seam by using ground vertical boreholes. *Rock Soil Mech.* **2019**, *40*, 370–378. [[CrossRef](#)]
40. Xiong, Y.W. Research progress on experimental methods for permeability characteristics of coal containing gas. *Saf. Coal Mines* **2018**, *49*, 184–188.
41. Lu, Z.J.; Li, S.Z. Experimental study on permeability and strain characteristics of coal containing gas. *Saf. Coal Mines* **2020**, *51*, 1–4.
42. Xue, W.T. Mechanism and Processes of Pore Gas Pressure Change of Gas Bearing Coal under Coupled Static-Dynamic Loads. Master's Thesis, China Coal Research Institute Health Center, Beijing, China, 2021.
43. Wang, H.P.; Zhang, Q.H.; Yuan, L.; Xue, J.H.; Li, Q.C.; Zhou, W.; Li, J.M.; Zhang, B. Development of a similar material for methane-bearing coal and its application to outburst experiment. *Rock Soil Mech.* **2015**, *36*, 1676–1682.
44. Xie, C.; Li, S.C.; Ping, Y.; Li, J.L.; Li, S.C. Study of nonlinear damage characteristics and numerical simulation of post-peak fractured rock mass. *Rock Soil Mech.* **2017**, *38*, 2128–2136. [[CrossRef](#)]
45. Tian, Z.C.; Tang, C.A.; Li, H.; Xing, H.; Ning, X.D. Numerical Simulation of Rock Uniaxial Compressive Strength and Deformation Failure Law under Different Size Conditions. *Adv. Civ. Eng.* **2021**, *2*, 1–11. [[CrossRef](#)]
46. Yu, C.; Gong, B.; Wu, N.; Xu, P.; Bao, X. Simulation of the Fracturing Process of Inclusions Embedded in Rock Matrix under Compression. *Appl. Sci.* **2022**, *12*, 8041. [[CrossRef](#)]
47. Tian, Z.C.; Tang, C.A.; Yu, C.T.; Liu, Y.J.; Chen, S.J.; Jin, Y. Shijiang Chen4 and Yun Jin. Numerical simulation analysis of mechanical properties on rock brittle-ductility transformation under different loading rates. *Front. Earth Sci.* **2022**, *7*, 1–15. [[CrossRef](#)]